

THE LUMINOSITY FUNCTIONS OF SOME HALO GLOBULAR CLUSTERS

J. BORISSOVA, H. MARKOV, N. SPASSOVA

*Institute of Astronomy, Bulgarian Academy of Sciences
72 Tzarigradsko Chaussee Blvd., BG-1784 Sofia, Bulgaria*

Received 9 February 1996

Abstract. The luminosity functions of the brighter part of the color-magnitude diagram of some halo clusters: Pal1, Pal4, Pal13 and NGC6229 are obtained. Some cluster parameters such as helium abundance, metallicity and age are determined. A search for the so-called "RGB-bump" was made and the bump was detected in Pal4 and possibly in Pal13.

1. Introduction

Star counts in Galactic globular clusters (GC) provide observational input into a large variety of astrophysical problems. The photometry and counting of stars in different evolutionary phases presented in a color-magnitude (CM) diagram offer an unique opportunity of testing the stellar evolution theory when the observed luminosity functions (LF) are compared with the theoretical lifetimes. The cluster LFs, along the cluster main sequence are directly related to the stellar mass function and yield insight into the star formation scenarios of the early universe. In the last years a great number of the investigations were concentrated on the counts of main sequence stars, i. e. the stars that have small masses (down to $0.15 M_{\odot}$). The star counts of the stars up to the turnoff point are available from old work based on the photographic plates and "by-eye" counts mainly.

The purpose of our work is to construct the LFs of the brighter part of the color-magnitude diagram of some halo clusters using modern CCD detectors and a software able to dial star counts automatically.

2. Observations and Data Reduction

Observations of Pal1, Pal4, Pal13 and NGC6229 were made using the 2m RCC reflector of the Bulgarian National Astronomical Observatory. The obtained images were in the g and r passbands [8]. The frames were taken with the Focal Reduser of the Max Planck Institute for Aeronomy [5]. An EEV 576 x 385 CCD type P8603/B was used

as a detector. The telescope/reducer configuration and the CCD's square $22 \mu\text{m}$ pixels provide an image scale of 0.8 arcsec/px for an unvignetted field of about $7 \times 5 \text{ arcmin}$ at an effective focal ratio $f/2.86$. During the nights of observations the seeing was stable with measured stellar PSF on the raw frames about 1.5 FWHM arcsec .

The preliminary reductions of the CCD frames including bias subtraction and flat fielding were carried out using the standard MIDAS (ver. 92) data reduction package. Photometry of stars on the frames was performed using the point-spread function (PSF) fitting package DAOPHOT [7]. The conversion from instrumental (g_i, r_i) to standard (g, r) magnitudes was based on the standard stars from the list of Thuan and Gunn [8].

Table 1. Luminosity Functions of Pal1, Pal4, Pal13 and NGC6229

g	N_{Pal1}	N_{Pal4}	N_{Pal13}	N_{NGC6229}
16.25	5	--	--	26
16.75	2	--	--	43
17.25	4	--	5	74
17.75	4	--	4	100
18.25	8	3	1	167
18.75	15	2	5	146.9
19.25	11.84	1	4	117.7
19.75	32.15	10	12.25	148.1
20.25	17.59	7	27.96	191.2
20.75	16.55	30	44.94	--
21.25	35.66	7	48.78	--
21.75	--	5	--	--
22.25	--	7.14	--	--
22.75	--	16.13	--	--
23.25	--	29.21	--	--
23.75	--	44.82	--	--

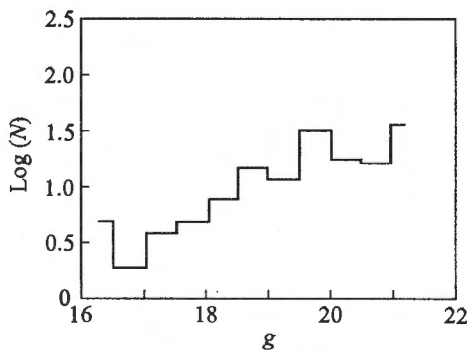


Fig. 1. Luminosity function of Pal 1 members in g band

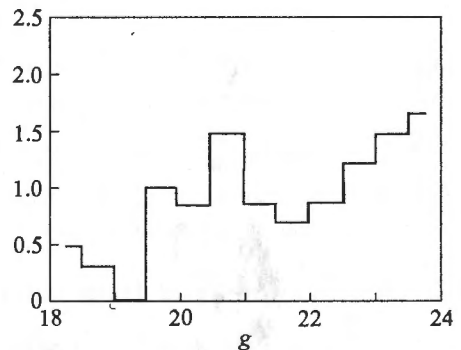


Fig. 2. Luminosity function of Pal 4 members in g band

3. Luminosity Functions

Completeness, photometric accuracy and subtraction of field stars are among the main problems in constructing the observed luminosity function. We followed method described in [2] to obtain the corrected LFs of Pal1, Pal4, Pal13 and NGC6229. For each individual cluster we have: (i) obtained CMD, (ii) corrected for completeness, (iii) de-contaminated cluster members from field stars. Table 1 lists the LFs of Pal1, Pal4, Pal13 and NGC6229. Column 1 lists the mean magnitude in g filter adopted for each bin. Columns 2, 3, 4 and 5 contain the observed LF corrected for completeness and field stars for Pal1, Pal4, Pal13 and NGC6229 respectively.

The LF of Pal1 is shown in Fig. 1. The two peaks located at $g = 16.50$ and $g = 19.50$ correspond to the positions of the horizontal branch and main sequence turnoff. A certain deficiency of stars can be observed from about 0.5 mag below the turnoff down to 21 mag. The LF of Pal4 is shown in Fig. 2. The peak located at $g = 20.5$ corresponds to the position of the horizontal branch stars. The LF of Pal13 is shown in Fig. 3. A certain deficiency of stars can be observed at $g = 18$ mag due to the sparsely populated RGB. The LF of NGC6229 is shown in Fig. 4. The peak located at $g = 18$ corresponds to the position of the horizontal branch stars. A significant deficiency of stars can be observed from about $g = 19$.

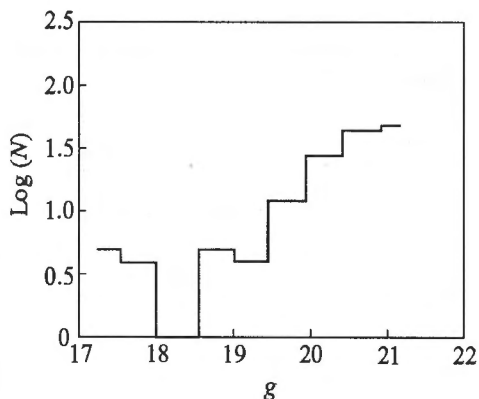


Fig. 3. Luminosity function of Pal 13 members in g band

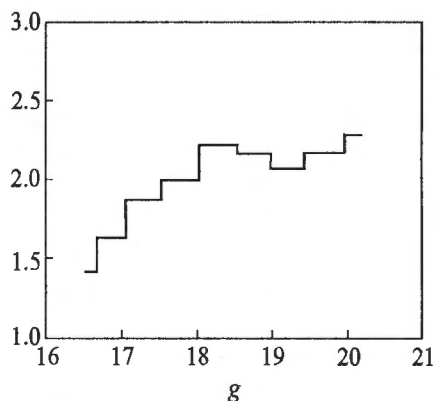


Fig. 4. Luminosity function of NGC6229 members in g band

From the observed LFs we can obtain the following information:

1. The LF for the unevolved main sequence yields the slope of the initial mass function.
2. The observed LFs are sensitive to the helium abundance, metallicities and age.
3. The LFs of the giant branch can help us to search for some features — gaps and peaks, which are predicted by standard stellar theory.

Unfortunately our data extend only slightly below the main sequence turnoff point. They cannot therefore be used to address the question of the clusters initial mass function.

Table 2. Derived cluster parameters

Cluster	$M(V)_{\text{TO-SGB}}$ observed	$\log(N)_{\text{TO-SGB}}$ observed	$\log(N)_{\text{TO-SGB}}$ predicted	[Fe/H]	[O/Fe]	Y	Age Gyr
Pal1	3.8	2.1	2.16	-1.03	0.50	0.2368	14
Pal4	3.8	2.1	2.12	-1.26	0.55	0.2358	14
Pal13	4.2	2.3	2.32	-1.48	0.60	0.2354	12
NGC6229	4.0	2.2	2.21	-1.48	0.60	0.2354	14

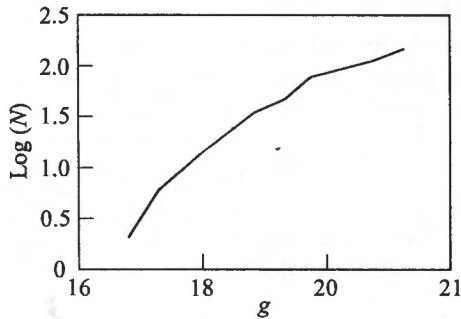


Fig. 5. Cumulative luminosity function of Pal 1 determined without horizontal branch stars

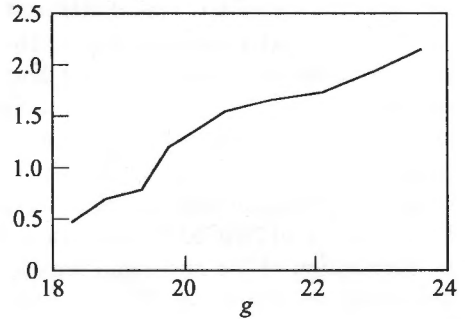


Fig. 6. Cumulative luminosity function of Pal 4 determined without horizontal branch stars

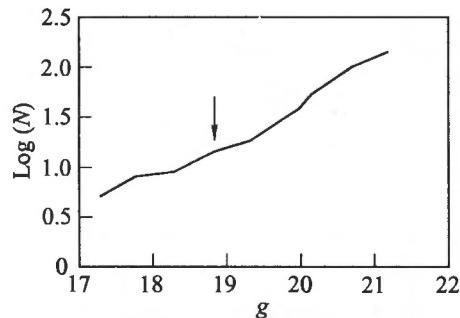


Fig. 7. Cumulative luminosity function of Pal 13 determined without horizontal branch stars

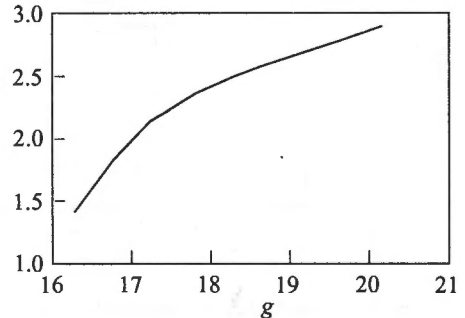


Fig. 8. Cumulative luminosity function of NGC6229 determined without horizontal branch stars

. From the turnoff point to the tip of the giant branch the LF is insensitive to the initial mass function and to the effects of mass segregation because the range in mass is very small ($< 0.3 M_{\odot}$). The location of the region in the LF, just above the main sequence turnoff point, is mainly age sensitive, while the slope of the region is sensitive to metallicity and helium content. By comparison between a value of the LFs in the turnoff-to-subgiant region with that predicted from theoretical luminosity functions computed by Bergbusch and Vandenberg [1] we obtained the following parameters

— metallicity — $[Fe/H]$ and $[O/Fe]$, helium content — Y and age. The parameters are summarized in Table 2. All LFs were normalized to give the same number of stars ($N = 10$) at $M_V = 2$. The corresponding values from [3] are consistent with our estimate. The cumulative LFs of Pal1, Pal4, Pal13 and NGC6229 determined without horizontal branch stars (HB stars are in different state of evolution) are shown in Figs 5, 6, 7 and 8.

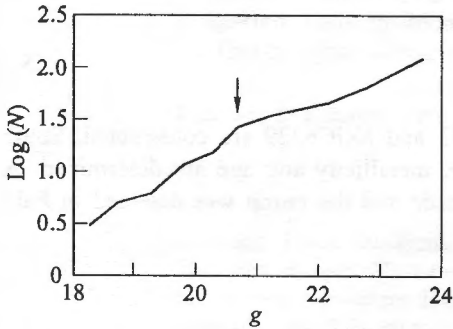


Fig. 9. Observed luminosity function of Pal 4 determined for red giant branch stars

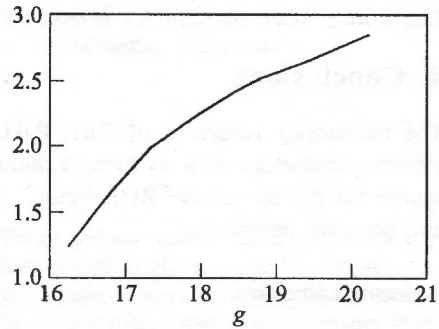


Fig. 10. Observed luminosity function of NGC6229 determined for red giant branch stars

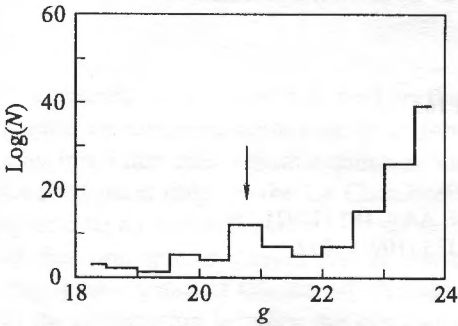


Fig. 11. Differential luminosity function of Pal 4 determined for red giant branch stars

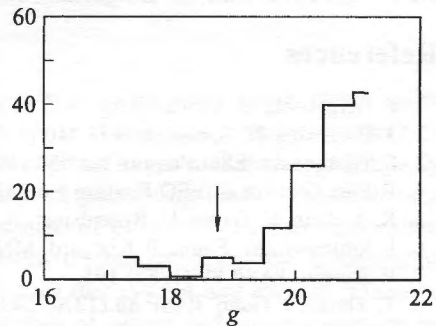


Fig. 12. Differential luminosity function of Pal 13 determined for red giant branch stars

In standard stellar models, at some point of the lower part of the RGB the convective envelope penetrates deep enough into the star to reach of varying hydrogen abundance established during core hydrogen-burning. When the convective envelope retreats from the advancing H-burning shell, a discontinuity in the H-profile is left. Eventually the H-burning shell passes through this discontinuity leading to a potentially observable bump in the LF. Figs 7, 9 and 10 show the observed LFs used to detect the RGB-bump. For each individual cluster we have separated RGB stars from HB and AGB objects. At Pal1 we do not found the stars in phase of evolution corresponding to the red giants, the brightest stars in the cluster are the HB stars so we can exclude this cluster. At

Pal13 we do not found stars in AGB phase of evolution and RGB is very sparsely populated. The Pal4 and NGC6229 have well defined RGBs. Following the method described by Fusi Pecci et al. [4] we have searched for the break in the slope at the cumulative LFs. The RGB-bump cannot be detected in the NGC6229 (see Fig. 10). In Pal4 the break is detected at $g = 20.75$. In Fig. 11 we show the differential LF, when the RGB-bump is more obvious. In Pal13 we can detect some break at $g = 18.50$. In Fig. 12 we show the differential LF. But the number of stars in RGB of Pal13 is small and more precise photometry is necessary to confirm this.

4. Conclusions

The luminosity functions of Pal1, Pal4, Pal13 and NGC6229 are constructed. Some cluster parameters such as helium abundance, metallicity and age are determined. A search for the so-called "RGB-bump" was made and the bump was detected in Pal4 and possibly in Pal13.

Acknowledgments

The authors are grateful to Dr. Jokers from the Max Planck Institute for Aeronomy for the opportunity to use their Focal Reduser and CCD camera and to Dr. Bonev who helped us in the process of acquiring the CCD data.

This research was supported by the Bulgarian National Science Fund under contract No F-328/1993 with the Bulgarian Ministry of Education and Science.

References

1. P. Bergbusch, D. Vanden Berg. *AAS* **81** (1992) 163.
2. J. Borissova, N. Spassova. *AAS* **110** (1995) 1.
3. S. Djorgovski. ESO Preprint No 932 (1993) 32.
4. F. Fusi Pecci et al. ESO Preprint No 687 (1989).
5. K. Jockers, E. Gayer, H. Rosenbauer, A. Hanal. *A&A* **187** (1992) 256.
6. I. Jorgensen, M. Franx, P. Kjargard. *MNRAS* **273** (1095) 1097.
7. P. Stetson. *PASP* **99** (1987) 191.
8. T. Thuan, J. Gunn. *PASP* **88** (1976) 543.